ILASS Americas, 24th Annual Conference on Liquid Atomization and Spray Systems, San Antonio, TX, May 2012

Particle Size and Velocity Measurements using Light-Field Velocimetry

T. Nonn*, V. Jaunet, C. Weissman
Dantec Dynamics A/S
2740 Skovlunde, Denmark

Abstract

The last few years have seen considerable activity regarding light-field cameras and their application to photography. The ability to refocus images over a finite depth range has consequently led to interest in measuring the distance of objects from the camera. While originally developed for imaging textured opaque surfaces, interest has led to successful application in volumetric flow-fields using a commercially developed plenoptics camera. It is then expected that once particles are successfully imaged in 3D PIV flows, 2-phase and spray flows naturally follow. This paper focuses on measurement of spray particle flow velocity and size using a single light-field camera. While previous techniques utilised a limiting 2D shadowing technique, measuring the size and velocity of particles silhouetted from behind with uniform illumination, light-field measurements open the possibility of accessing the depth position, and thus the 3D position and velocity of individual bubbles and droplets.

*Corresponding author: thomas.nonn@dantecdynamics.com

Introduction

The light-field (LF) technique has been described widely in literature [1,2,3], having its origins more than a century ago, but only in the last decade has momentum behind the technique increased, due to advances in optics, sensor resolution and manufacturing techniques. Currently the measurement of three-dimensional velocity components in experimental flow setups is carried out using multiple cameras, positioned around a fixed point and carefully aligned and calibrated. A single light-field camera opens up the possibility of a low-cost, robust and flexible alternative to multiple camera 3D measurement systems. A single camera capturing 3D events simplifies both physical access and calibration.

The general principle behind light-field camera can be described as follows: a micro-lens array placed closely to an image sensor, with the same f-stop as the main objective, reconstructs at selected positions virtual images representing focus planes within the measurement volume, as shown in figure 1.

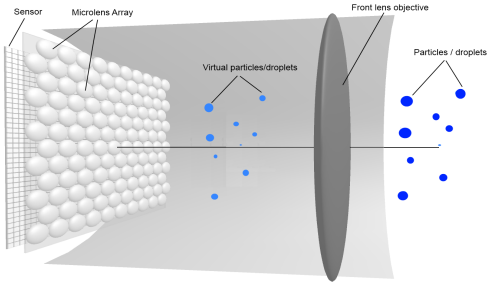

Figure 1. Optical schematic of light-field principle.

Particles appear in micro-images within several micro-lenses, at slightly different perspectives, allowing for depth determination. The downside of light-field cameras, however, is the loss of spatial resolution. The loss can be mitigated by applying multiple-focus micro-lens techniques used by a commercially available plenoptics

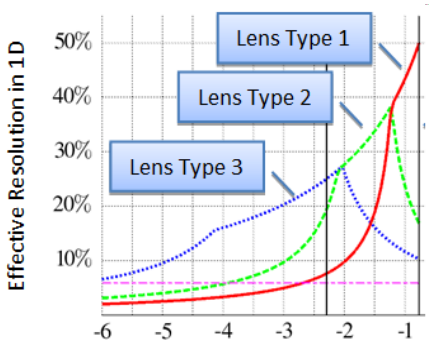

Figure 2. Resolution versus depth (courtesy Raytrix)

camera. In the worst case (near-field) roughly 25 percent of the spatial resolution is retained, thus the 11 MP camera used in this study had an effective resolution of 2.6 MP. The depth resolution through the measurement volume is not constant, but increases monotonically with distance from the main objective, reaching a maximum in the far-field, as seen in figure 2.

Neighbouring micro-lenses act as local stereo systems, imaging large particles such as bubbles or droplets at slightly different perspectives, disclosing not only position in 3D space, but surface features as well. The depth of field of a light-field camera, or measurement depth, is limited by the f-stop of the microlens, which is also the f-stop of the main objective. Exploiting a micro-lens array (MLA) with multiple focal lengths, the depth of field can be extended, up to a factor of seven with three focal lengths. Figures 3 and 4 compare the imaging of seeding particles and droplets on the micro-lenses. Note that in the micro-lens images below the degree of defocusing varies from lens to lens. Due to the hexagonal arrangement of the micro-lenses, no two lens of the same focal length are ever in contact. Images from lenses with the same focal lengths are examined together and compared against results from the other lens types.

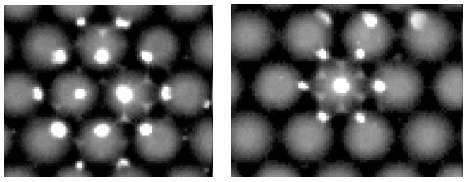

Figure 3. Near-field and far-field images of a 30 micron spherical particle.

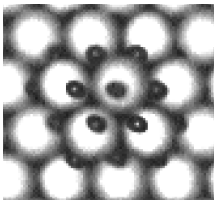

Figure 4. Micro-lens image of a droplet in a spray..

As in PIV, the determination of the velocity field of particles in a volume requires the acquisition of at minimum two light-field images acquired in rapid succession. The depth map determined for each image is then analysed individually for particle positions and then processed together to determine the velocity field and particle flow history. Depending on the operating mode of the camera used the velocity field can the be

determined from particle tracking techniques, least-square methods (LSM) or three-dimensional cross-correlation techniques. In practice the light-field camera operates best in flows with low to medium seeding densities. In higher densities particles become difficult to resolve and occlusion makes tracking difficult.

For particle size measurements the particles need to be sufficiently large so that the reconstructed focus images produce particle images that can be analyzed by conventional edge detection techniques.

Experimental setup

The investigation consisted of measuring droplets from a aerated spray nozzle typically found in agriculture. A Raytrix light-field camera used in combination with a Dantec imaging system was used for acquisition of data. Illumination was provided by a pulsed shadow strobe combined with a diffuser. For comparison purposes, 2D measurements on the nozzle were also carried with a phase-Doppler (PDA) system.

The imaging system was calibrated with a textured dot target commonly used in stereo PIV. The calibration process consists of three independent processes: (1) software alignment of the micro-lens array (MLA); (2) calibration of the depth space based on the pinhole model; (3) Matching of the depth response of the light-field camera with the depth determined from the target calibration. The entire calibration process consists of acquiring two images: a target image and a white image. The calibration target is placed diagonally across the measurement volume. The focus is adjusted so that dots farthest from the camera are nearly in focus. As one moves to the near-field dots begin to occupy ever larger rings of lenses. The depth volume depends on the focal length of the objective selected and the working distance

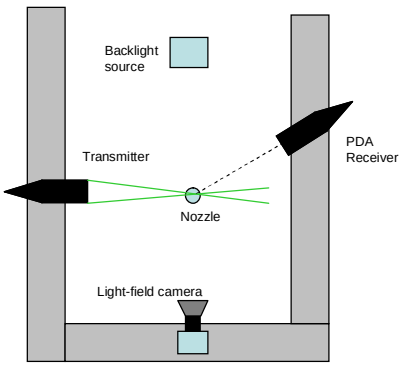

Figure 5. Layout of spray experiment.

The alignment process ensures that the lenses are properly specified in the software during the reconstruction of the focus images. The near-field lenses were heavily vignetted (i.e. defocused). The next step in the calibration requires that the object to image coordinate relationship be determined. An interesting property of light-field technology is the so-called "all-in-one" focus. Instead of focusing on a particular plane the depth map determined from the light-field data is used to put all objects in an image in focus. In this case all of the dots on the target are focused. This image is then processed using a pinhole camera model to extract a transformation between image and object space. This essentially contains all our scaling information for 3D measurements. Typical reprojection errors were on the order of 0.5 - 0.8 pixels. It is expected that this uncertainty can be improved using a specially designed target with a finer dot distribution.

The last step of the calibration involves matching the virtual depth values returned by the camera with the actual depth values determined by the camera model. It was found for longer focal length objectives (> 100 mm) the relationship between virtual depth and actual depth was approximately linear, as is evident in figure 6. For shorter focal length lenses the relationship was parabolic. Once the calibration procedure is complete the target used can be reconstructed in 3D as verification (figure 7). Typical residuals for the fit were between 0.5 - 1.0 %.

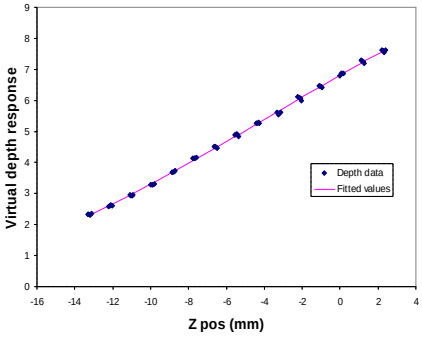

Figure 6. Calibration fit between virtual depth and measured depth**.**

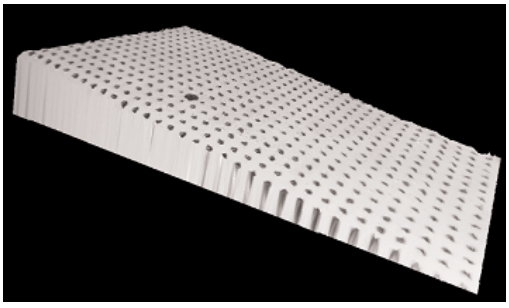

Figure 7. 3D Reconstruction of calibration target**.**

Results

For the current investigation a series of images was taken of the entire spray. Thereafter, several runs of 200 images were acquired from a subset of the whole field using the light-field camera, as shown in figures 8 and 9. In the subset ROI roughly 10-15 droplets were captured in each image. The working volume of the ROI subset was 3.8 cm x 2.5 cm x 1.4 cm. The minimum diameter that could be effectively evaluated with the current optical setup was 10 microns. A higher resolution camera would have assisted in recovering more of the smaller droplets. A series of measurements with a PDA (phase-Doppler) system were carried out over the entire spray. Two vertical slices of the volume giving 32 positions in total were used for comparisons. An example is given in Figure 10 comparing diameter distributions between the PDA and LF system.

A time-averaged result of the ROI data sequence, figure 11,shows the characteristic distribution of larger droplets in the outer region of the spray cone and the gradual falling off toward the center of the spray.

Conclusion

This investigation introduces the light-field camera to 3D spray measurement. It could be seen that not only droplets are useful subjects of this technology, but that the depth measurement could also determine positions of structures such as ligaments and the sheath of the spray.

In general, the light-field camera simplifies the measurement and calibration process for 3D analysis. Another added value of LF over the shadow measurement technique is in resolving out-of-focus particles, a persistent problem for conventional imaging. The investigation also focused on the uncertainties involved with LF measurement. This work is still preliminary and reconstruction of the results in a 3D format remains to be done. However, these early results show promise and point to the practical usefulness of light-field technology in 3D measurement.

References

1. T. Nonn, J. Kitzhofer and D. Hess, "Measurements in an IC-engine Flow using Light Field Volumetric Velocimetry", *Laser Appl. Fluid Flows*, Lisbon 2012.
2. M. Levoy, "Light fields and computational imaging," Computer, vol. 39, pp. 46-55, 2006.
3. R. Ng, M. Levoy, M. Bredif, G. Duval, M. Horowitz, and P. Hanrahan, "Light field photography with a hand-held plenoptic camera," tech. rep., Stanford University, 2005
4. Haeyoung Jeong, Kihyung Lee and Yuji Ikeda, "Investigation of the spray characteristics for a secondary fuel injector using a digital image processing method", Measurement Science and Tech.", vol. 18, pp.1591-1602, 2007.

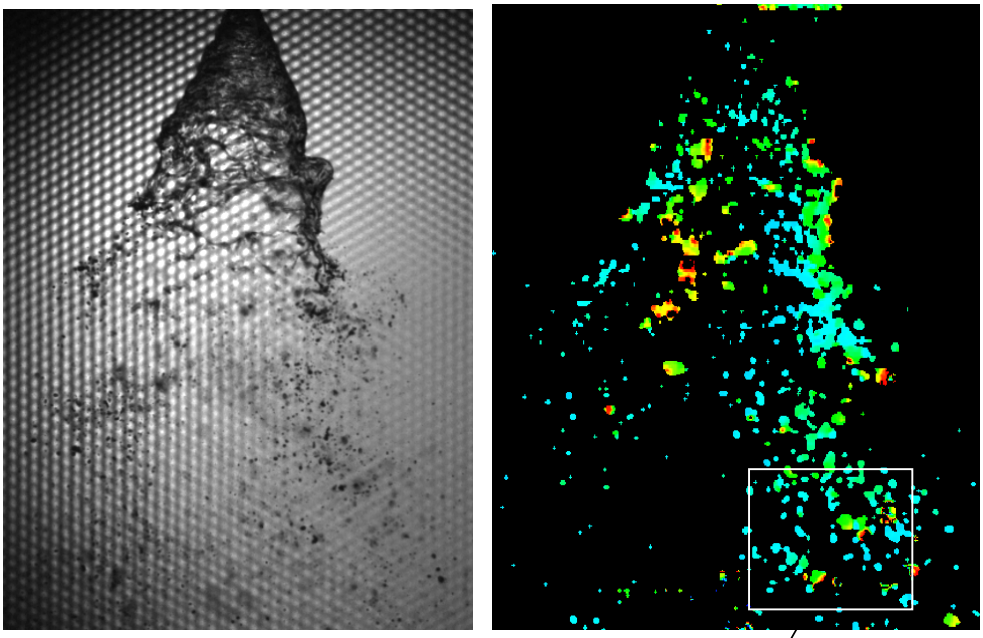

Figure 8. Focus and color-mapped depth map of spray from light-field results.

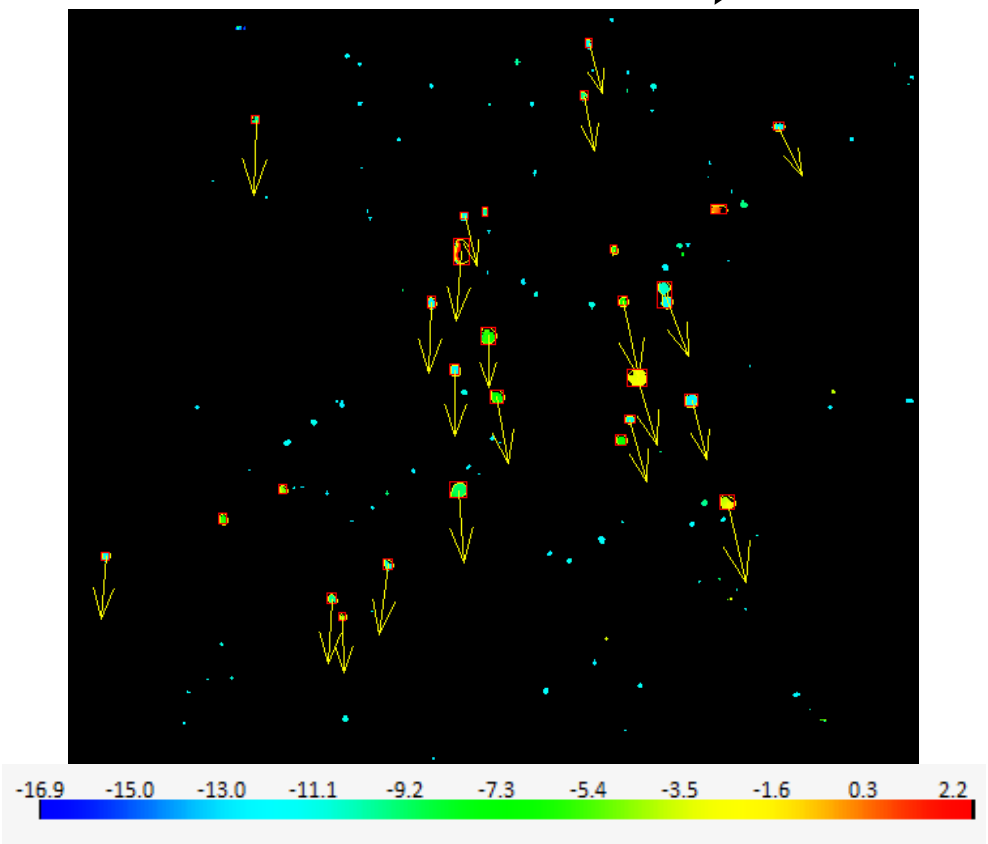

Figure 9. Subset ROI of spray with color mapped depth and 2D vectors.

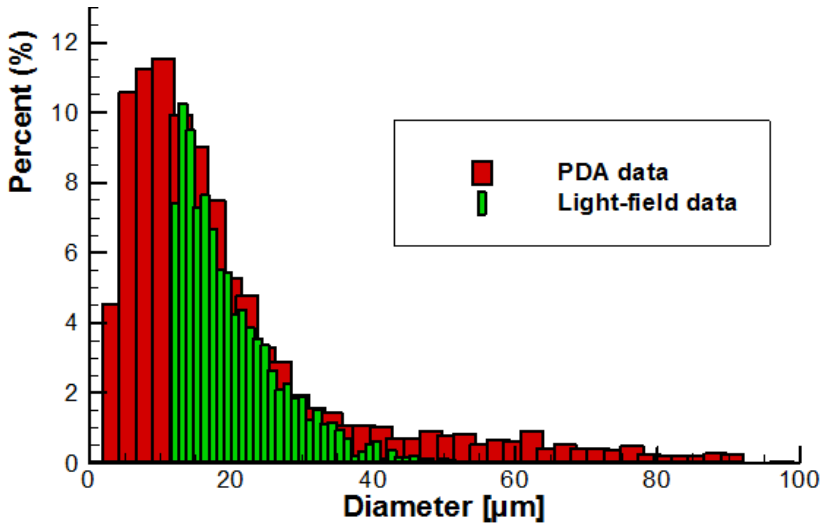

Figure 10. Comparison of spray particle diameter distributions between data acquired from PDA and Light-field camera.

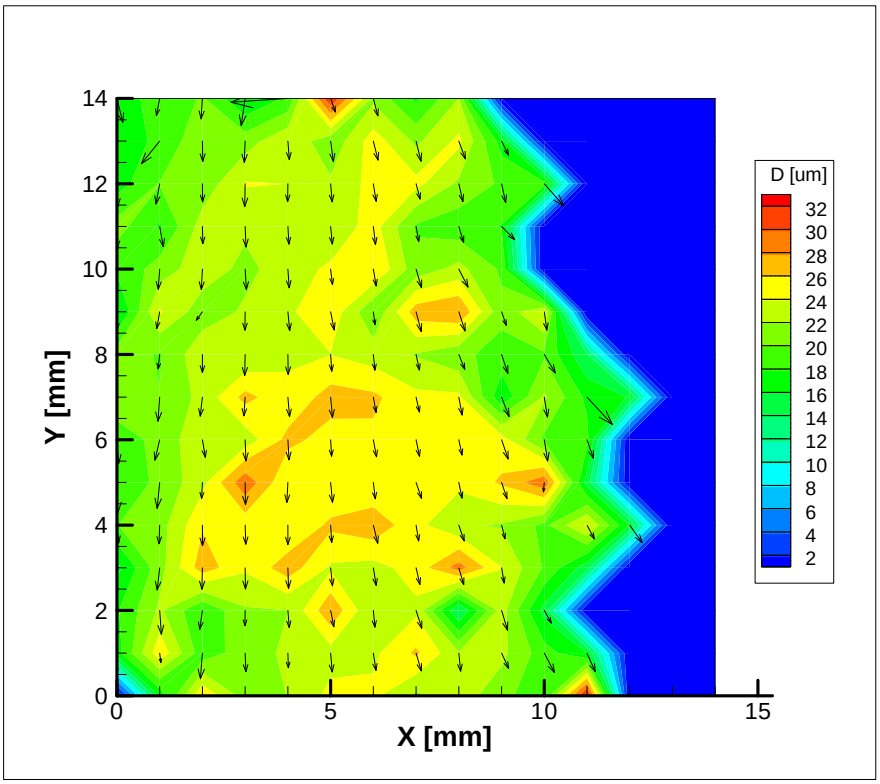

Figure 11. Time-averaged velocity and diameter data (200 images).